Bioorganic Chemistry 91 (2019) 103171

Contents lists available at ScienceDirect

Bioorganic Chemistry

journal homepage: www.elsevier.com/locate/bioorg

Discovery, synthesis and molecular substantiation of N-(benzo[*d*]thiazol-2-yl)-2-hydroxyquinoline-4-carboxamides as anticancer agents

B. Bindu[a], S. Vijayalakshmi[a,**], A. Manikandan[b,*]

[a] Dept. of Chemistry, Government Arts College, Coimbatore 641018, Tamil Nadu, India
[b] Dept. of Biotech, School of Biosciences and Technology, VIT University, Vellore 632014, Tamil Nadu, India

ARTICLE INFO

Keywords:
Alkaline phosphatase (ALP)
Anticancer
Benzothiazole
Carboxamide
Drug design
Molecular docking

ABSTRACT

The effort was taken to develop a series of benzothiazole and quinoline fused bioactive compounds obtained through a four-step synthetic route using a range of substituted acetoacetanilides. Achieved N-(benzo[*d*]thiazol-2-yl)-2-hydroxyquinoline-4-carboxamides (**6a-l**) were produced up to 96% of yield while the eco-friendly p-TSA used as a catalyst. Further, the anticancer activity of these compounds was determined using a range of cancer cell lines starting from MCF-7 (Breast cancer), HCT-116 (Colon cancer), PC-3 & LNCaP (Prostate) and SK-HEP-1 (Liver cancer). Present study compounds were also testified for antioxidant properties prior to anticancer studies since the Reactive Oxygen Species (ROS) being vital in cancer development. To determine the cell membrane stability effects of the compounds, human red blood cells (HRBC) based membrane protection assay was determined. In the results, compounds **6a-l** were able to produce a dominated result values over PC3 cell lines (Prostate cancer) than the other cell lines used in this study. Since the connectivity of human germ cell alkaline phosphatase (hGC-ALP) in the development of prostate cancer is known, the most active compounds were evaluated for the hGC-ALP inhibition in order to ensure a mechanism of anticancer action of these compounds. The mode of interaction and binding affinity of these compounds was also investigated by a molecular docking study. In the results, **6d, 6i, 6k,** and **6l** were found with least IC_{50} values < 0.075 μM and highest relative activity of 92%, 90%, and 96% respectively. The need for further animal model evaluation and pre-clinical studies recognized.

1. Introduction

Recognizing medicinally important molecules is an art in developing novel drugs against various diseases. Combinatorial approach is one of the effective way to screen most efficacious drug candidate from a range of derivatives designed from it. This study aimed to synthesis a family of 13 quinoline derivatives by using substituted acetoacetanilides to develop them as anticancer agents. Cancer is one of the most threatening diseases of this universe. Discovering effective drug is one of the most need of the hour. The present study aimed to prepare drug candidates in a combination with benzothiazole and quinoline. Numerous benzothiazole [1–3] and quinoline [4–6] based compounds and their derivatives are widely synthesized and testified for their biological activity potentials. Quinolines have demonstrated with a wide range of anticancer activities [7–9]. 2-phenylquinoline and 2-phenylquinolone derivatives have already been established as potent antitumor agents [10,11]. In their derivatives, quinoline ring takes significant responsibility in the mechanism of actions which are highly involving in the cancer developments like seizing cell cycle, cell migration distribution, angiogenesis inhibition, apoptosis, and in the nuclear receptor responsiveness modulations [12–14].

For example, imidazoquinoline skeleton in the 1,4-disubstituted imidazo[4,5-*c*]quinolines were found with excellent anti-cancer activity [15]. 2-phenyl quinoline comprising [(2-aminoethyl) aminomethyl] showed the capability of interpolation into double-stranded DNA which is an indispensable intention for cytotoxicity [16]. Initially, various substituted acetoacetanilides were treated with concentrated sulfuric acid to obtain corresponding quinolines. After two more steps, benzo[*d*]thiazol-2-amine was fused to achieve the target compounds N-(benzo[*d*]thiazol-2-yl)-2-hydroxyquinoline-4-carboxamides and relevant derivatives (**6a-l**) (Fig. 1). The successive bioactivity prediction was executed using the online bioactivity prediction tools such as Molinspiration (molinspiration.com) and PASSonline (pharmaexpert.ru/passonline/). As per the results displayed in Fig. 2, all compounds were

* Corresponding author.
** Corresponding author.
E-mail addresses: vijisomu@rediffmail.com (S. Vijayalakshmi), mailtomicromani@gmail.com (A. Manikandan).

https://doi.org/10.1016/j.bioorg.2019.103171
Received 5 June 2019; Received in revised form 24 July 2019; Accepted 30 July 2019
Available online 30 July 2019

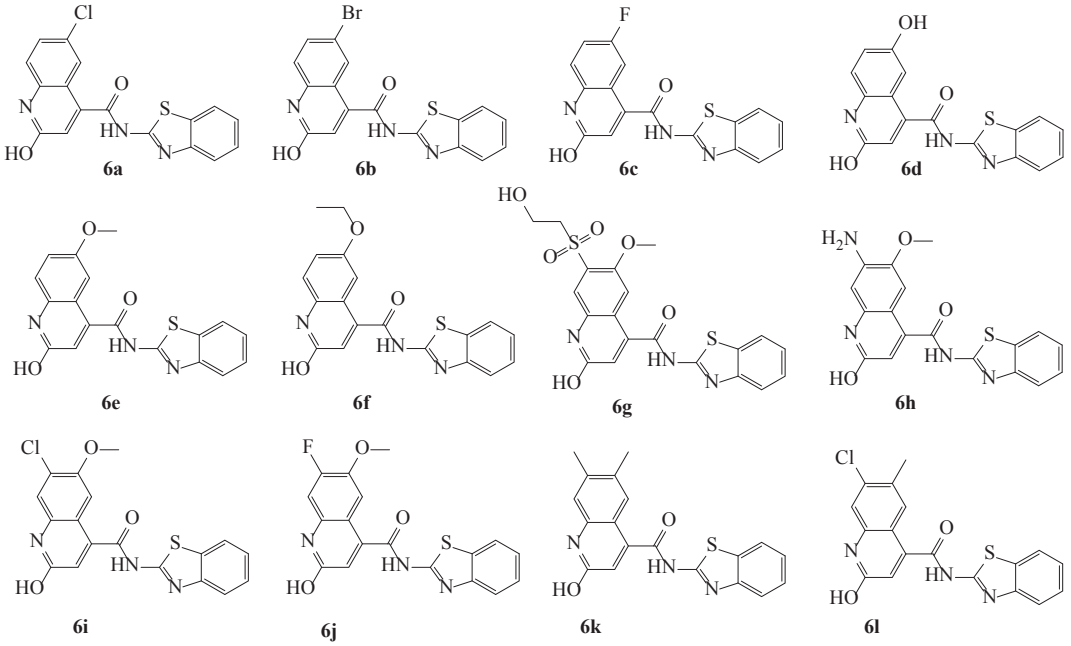

Fig. 1. Achieved final structures of present study compound N-(benzo[*d*]thiazol-2-yl)-2-hydroxyquinoline-4-carboxamides and relevant derivatives (**6a-l**).

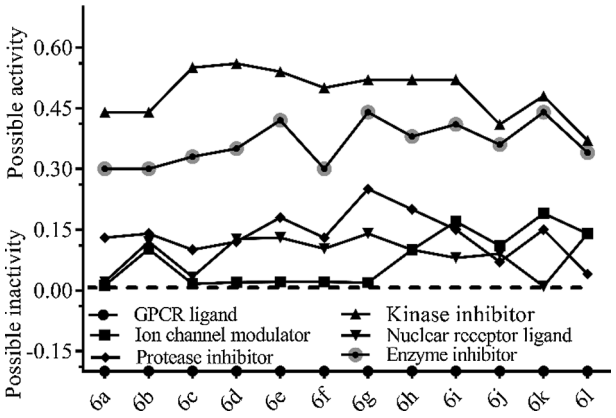

Fig. 2. Bioactivity prediction results of compounds **6a-l.**

showed a possible biological activity and the enzyme & kinase inhibition potential was the most favorable biological activity. As the prediction suggested, we aimed to develop the present study compounds as the protein-tyrosine kinase inhibitors and so as the anticancer agents.

2. Materials and methods

Chemistry: All organic chemicals and solvents were procured from Sigma-Aldrich, Merck and were used as received without further purification. Thin-Layer chromatography (TLC) was carried out using precoated silica plates (Merck-silica gel 60 F254). Merck silica gel 60 (230–400 mesh) was used for flash column chromatography. Melting point (mp) were checked using an OptiMelt automated melting point system and are uncorrected. ^{1}H and ^{13}C NMR spectra were recorded on Bruker spectrometer (400 & 100 MHz respectively) using $CDCl_3$ as the solvent. Tetramethylsilane was used as the internal standard. HRMS device (MS JOEL GC mate) used a secondary electron multiplier (Agilent Technologies 6890N Network GC system for gas chromatography) was used to record the MASS.

*2.1. General procedure for the preparation of N-(benzo[d]thiazol-2-yl)-2-hydroxyquinoline-4-carboxamides and relevant derivatives (**6a-l**)*

Substituted 3-oxo-*N*-phenylbutanamides (**1**) (0.012 mol) was added to concentrated sulfuric acid (0.001 mol) in portions on 75 °C to obtain substituted 4-methyl quinoline-2-ol (**2**) in an affordable yield range of 92–98%. To 1.5 g (0.0094 mol) of 4-methyl quinoline-2-ol (**2**) in water, 2.84 g (0.018 mol) of alk. $KMnO_4$ was added with stirring for 4 h and kept on the water bath for 2 h till the color of the mixture changes to brown. The reaction was then filtered and neutralized with 1:1 hydrochloric acid. The precipitate formed was washed with water and dried and recrystallized from hot water to obtain 2-hydroxyquinoline-4-carboxylic acid (**3**).

To 1 g (0.0053 mol) of 2-hydroxyquinoline-4-carboxylic acid (**3**), 0.077 ml (0.016 mol) oxalyl chloride was added and refluxed on a water bath. After the reaction excess oxalyl chloride was removed by co-distillation with benzene to obtain 2-hydroxyquinoline-4-carbonyl chloride (**4**). To 0.0054 mol of 2-hydroxyquinoline-4-carbonyl chloride (**4**) in ethanol 0.00464 mol of 2-aminobenzothiazole (**5**), 0.0082 mol and triethylamine were added and refluxed on a water bath for 6–8 h to obtain the title compound N-(benzo[*d*]thiazol-2-yl)-2-hydroxyquinoline-4-carboxamide (**6**).

*2.2. Characterization of N-(benzo[d]thiazol-2-yl)-2-hydroxyquinoline-4-carboxamides (**6a-l**)*

N-(benzo [*d*] thiazol-2-yl)-6-chloro-2-hydroxyquinoline-4-carboxamide (6a): Chalky white powder; Melting point: 124–126 °C: IR (KBr): 3242, 3066, 3098, 3028, 2915, 2874, 2333, 1738, 1586, 1464, 1430, 1387, 1265, 1212, 1118, 890, 754, 696, 674, 668, 642 cm^{-1}: ^{1}H NMR (400 MHz, $CDCl_3$) δ ppm: 12.91 (s, 1H), 11.58 (s, 1H), 9.02 (s, 1H), 8.36–8.20 (m, 3H), 7.93–7.91 (d, J = 8.0 Hz, 1H), 7.73 (s, 1H), 7.70–7.61 (m, 2H); ^{13}C NMR (100 MHz, $CDCl_3$) δ ppm: 178.6, 172.4, 168.0, 158.0, 150.4, 146.0, 143.3, 138.4, 136.8, 129.3, 128.7, 128.6, 128.4, 127.7, 127.5, 126.8, 126.7, 124.9, 123.9, 118.2, 115.5; Elemental Analysis, Calculated: C, 57.39; H, 2.83; Cl, 9.96; N, 11.81; S, 9.01; Obtained: C, 57.38; H, 2.84; Cl, 9.95; N, 11.82; S, 9.02. HRMS for $C_{17}H_{10}ClN_3O_2S$ Calculated [M^+] m/z 355.7960, Found 355.7962.

N-(benzo [*d*] thiazol-2-yl)-6-bromo-2-hydroxyquinoline-4-carboxamide (6b): White solid; Melting point: 128–130 °C: IR (KBr):

3332, 3116, 3028, 2908, 2864, 2333, 1739, 1588, 1466, 1432, 1378, 1266, 1234, 1108, 896, 758, 696, 672, 664 cm^{-1}: ^1H NMR (400 MHz, $CDCl_3$) δ ppm: 12.00 (s, 1H), 10.61 (s, 1H), 9.03 (s, 1H), 8.07–7.87 (m, 4H), 7.51 (s, 1H), 7.17–7.00 (m, 2H); ^{13}C NMR (100 MHz, $CDCl_3$) δ ppm: 178.7, 173.3, 167.7, 152.8, 151.7, 144.0, 143.9, 138.3, 137.9, 137.7, 137.3, 137.0, 128.8, 129.5, 126.0, 125.9, 125.7, 124.9, 122.8, 112.1, 110.1; Elemental Analysis: C, 51.01; H, 2.52; Br, 19.96; N, 10.50; S, 8.01; Obtained: C, 51.02; H, 2.53; Br, 19.96; N, 10.51; S, 8.02; HRMS for $C_{17}H_{10}BrN_3O_2S$ Calculated $[M^+]$ m/z 400.2500, Found 400.2500.

N-(benzo [*d*] thiazol-2-yl)-6-fluoro-2-hydroxyquinoline-4-carboxamide (6c): Pale yellow powder; Melting point: 120–122 °C: IR (KBr): 3296, 3018, 3002, 2919, 2860, 2342, 1818, 1742, 1566, 1430, 1370, 1264, 1234, 1119, 898, 758, 696, 674, 664, 642 cm^{-1}: ^1H NMR (400 MHz, $CDCl_3$) δ ppm: 12.06 (s, 1H), 10.32 (s, 1H), 8.88 (s, 1H) 8.26–8.25 (d, J = 8.0, 1H), 8.24–8.04 (m, 2H), 7.96 (s, 1H), 7.94–7.82 (m, 2H), 7.66–7.63 (t, J = 12, 1H); ^{13}C NMR (100 MHz, $CDCl_3$) δ ppm: 178.9, 174.9, 168.9, 154.0, 152.9, 145.2, 145.1, 139.4, 139.1, 138.9, 138.5, 138.2, 131.0, 130.6, 127.2, 127.1, 126.9, 126.1, 124.0, 113.3, 103.4; Elemental Analysis: C, 60.17; H, 2.97; F, 5.60; N, 12.38; S, 9.45; Obtained: C, 60.19; H, 2.98; F, 5.60; N, 12.39; S, 9.46; HRMS for $C_{17}H_{10}FN_3O_2S$ Calculated $[M^+]$ m/z 339.3444, Found 339.3445.

N-(benzo [*d*] thiazol-2-yl)-2,6-dihydroxyquinoline-4-carboxamide (6d): Chalky white powder; Melting point: 124–126 °C: IR (KBr): 3301, 3187, 3023, 2984, 2862, 2318, 1734, 1586, 1464, 1430, 1342, 1265, 1224, 1118, 884, 762, 698, 664, 652, 646 cm^{-1}: ^1H NMR (400 MHz, $CDCl_3$) δ ppm: 12.90 (s, 1H), 11.64 (s, 1H), 8.73 (s, 1H), 8.49 (s, 1H), 8.31–8.28 (t, J = 8.0, 1H), 8.20–8.17 (t, J = 8.0 Hz, 1H), 7.91–7.90 (d, J = 8.0, 1H), 7.78–7.68 (m, 3H), 7.32–7.31 (d, J = 8.0, 1H); ^{13}C NMR (100 MHz, $CDCl_3$) δ ppm: 176.7, 172.7, 167.7, 152.9, 151.7, 144.1, 144.0, 138.3, 137.9, 137.7, 137.4, 128.8, 129.5, 126.0, 125.9, 125.8, 124.9, 122.8, 112.2, 102.2; Elemental Analysis: C, 60.53; H, 3.29; N, 12.46; S, 9.50; Obtained: C, 60.55; H, 3.29; N, 12.47; S, 9.50; HRMS for $C_{17}H_{11}N_3O_3S$ Calculated $[M^+]$ m/z 337.3530, Found 337.3533.

N-(benzo [*d*] thiazol-2-yl)-2-hydroxy-6-methoxyquinoline-4-carboxamide (6e): Ash color solid; Melting point: 126–128 °C: IR (KBr): 3340, 3186, 3088, 3021, 2918, 2866, 2331, 1734, 1586, 1464, 1432, 1387, 1265, 1213, 1118, 894, 754, 696, 674, 664, 641 cm^{-1}: ^1H NMR (400 MHz, $CDCl_3$) δ ppm: 12.17 (s, 1H), 11.79 (s, 1H), 8.88 (s, 1H), 8.54–8.49 (t, J = 8.0, 1H), 8.35–8.33 (t, J = 6.8, 1H), 8.21–8.19 (d, J = 8.0 Hz, 1H), 7.73–7.61 (m, 3H), 7.42–7.40 (d, J = 8.0, 1H), 3.83 (s, 3H); ^{13}C NMR (100 MHz, $CDCl_3$) δ ppm: 179.0, 177.4, 169.9, 164.3, 164.2, 161.9, 161.7, 155.7, 147.0, 146.4, 145.5, 137.6, 130.2, 129.7, 129.0, 126.0, 125.7, 122.1, 116.7, 114.2, 113.7, 112.9, 97.5, 54.8; Elemental Analysis calculated: C, 61.53; H, 3.73; N, 11.96; S, 9.12; Obtained: C, 61.53; H, 3.72; N, 11.97; S, 9.13; HRMS for $C_{18}H_{13}N_3O_3S$ Calculated $[M^+]$ m/z 351.3800, Found 351.3800.

N-(benzo [*d*] thiazol-2-yl)-6-ethoxy-2-hydroxyquinoline-4-carboxamide (6f): White powder; Melting point: 132–134 °C: IR (KBr): 3241, 3064, 3086, 3012, 2976, 2832, 2336, 1748, 1502, 1463, 1432, 1387, 1265, 1234, 1118, 890, 754, 692, 678, 646 cm^{-1}: ^1H NMR (400 MHz, $CDCl_3$) δ ppm: 13.23 (s, 1H), 11.14 (s, 1H), 8.55 (s, 1H), 7.94–7.71 (m, 2H), 7.69–7.62 (m, 1H), 7.55–7.54 (d, J = 8.0 Hz, 1H), 7.46–7.38 (m, 2H), 7.17–7.15 (d, J = 8.0, 1H), 3.75–3.70 (m, 2H), 1.80–1.72 (t, J = 8.0, 3H); ^{13}C NMR (100 MHz, $CDCl_3$) δ ppm: 178.2, 173.2, 168.2, 156.0, 147.1, 141.1, 139.7, 138.0, 136.5, 135.7, 129.2, 128.9, 128.8, 128.7, 126.5, 126.3, 125.7, 125.5, 116.0, 112.9, 98.4, 59.6, 14.81; Elemental Analysis, calculated: C, 62.45; H, 4.14; N, 11.50; S, 8.77; Obtained: C, 62.43; H, 4.16; N, 11.50; S, 8.76; HRMS for $C_{19}H_{15}N_3O_3S$ Calculated $[M^+]$ m/z 365.4070, Found 365.4072.

N-(benzo [*d*] thiazol-2-yl)-2-hydroxy-7-((2-hydroxyethyl)sulfonyl)-6-methoxyquinoline-4-carboxamide (6g): White solid; Melting point: 148–150 °C: IR (KBr): 3324, 3192, 3084, 3012, 2964, 2827, 2342, 1734, 1574, 1418, 1402, 1386, 1234, 1208, 1107, 894, 758, 696, 664 cm^{-1}: ^1H NMR (400 MHz, $CDCl_3$) δ ppm: 12.94 (s, 1H), 11.18 (s, 1H), 8.94 (s, 1H), 8.54–8.53 (d, J = 4, 1H), 7.99–7.94 (m, 2H), 7.37–7.26 (m, 3H), 4.37 (s, 1H), 3.75–3.71 (t, J = 8.0, 2H), 3.37 (s, 3H), 3.16–3.02 (t, J = 8.0, 2H); ^{13}C NMR (100 MHz, $CDCl_3$) δ ppm: 177.9, 172.7, 167.7, 155.7, 146.5, 142.5, 140.9, 137.7, 132.8, 132.1, 129.0, 129.0, 128.7, 128.4, 128.0, 127.8, 125.9, 125.6, 116.7, 113.0, 97.8, 59.8, 55.0, 54.7; Elemental Analysis, calculated: C, 52.28; H, 3.73; N, 9.15; S, 13.95; Obtained: C, 52.29; H, 3.72; N, 9.16; S, 13.96; HRMS for $C_{20}H_{17}N_3O_6S_2$ Calculated $[M^+]$ m/z 459.4910, Found 459.4913.

7-amino-N-(benzo [*d*] thiazol-2-yl)-2-hydroxy-6-methoxyquinoline-4-carboxamide (6h): Yellow solid; Melting point: 128–130 °C: IR (KBr): 3214, 3065, 2964, 2876, 2345, 1789, 1618, 1543, 1427, 1327, 1266, 1223, 996, 864, 654, 674, 668, 648 cm^{-1}: ^1H NMR (400 MHz, $CDCl_3$) δ ppm: 12.58 (s, 1H), 11.25 (s, 1H), 8.41–8.39 (m, 1H), 8.09–8.07 (m, 1H), 7.82 (s, 1H), 7.65–7.63 (m, 2H), 7.40 (s, 1H), 6.88 (s, 1H), 5.58, (s, 2H), 3.77 (s, 3H); ^{13}C NMR (100 MHz, $CDCl_3$) δ ppm: 178.3, 173.7, 168.3, 156.2, 147.1, 143.2, 142.0, 141.2, 140.1, 138.0, 128.8, 128.7, 128.1, 127.7, 126.6, 126.3, 125.9, 125.6, 115.9, 112.9, 98.3, 58.1; Elemental Analysis, calculated: C, 59.01; H, 3.85; N, 15.29; O, 13.10; S, 8.75; Obtained: C, 59.01; H, 3.85; N, 15.29; S, 8.75; HRMS for $C_{18}H_{14}N_4O_3S$ Calculated $[M^+]$ m/z 366.3950, Found 366.3951.

N-(benzo [*d*] thiazol-2-yl)-7-chloro-2-hydroxy-6-methoxyquinoline-4-carboxamide (6i): Yellow solid; Melting point: 124–126 °C: IR (KBr): 3256, 3048, 3018, 3002, 2948, 2866, 2334, 1724, 1524, 1468, 1432, 1388, 1268, 1234, 1108, 898, 756, 696, 674, 664, 642 cm^{-1}: ^1H NMR (400 MHz, $CDCl_3$) δ ppm: 12.79 (s, 1H), 11.11 (s, 1H), 8.37 (s, 1H), 8.13 (s, 1H), 8.10–7.90 (m, 1H), 7.63 (s, 1H), 7.48–7.38 (m, 3H), 3.80 (s, 3H); ^{13}C NMR (100 MHz, $CDCl_3$) δ ppm: 177.7, 173.0, 166.7, 154.6, 145.5, 141.5, 140.4, 139.6, 138.5, 136.4, 127.2, 126.0, 125.0, 124.0, 114.3, 111.3, 96.7, 53.2; Elemental Analysis, calculated: C, 56.04; H, 3.14; Cl, 9.19; N, 10.89; S, 8.31; Obtained: C, 56.05; H, 3.14; Cl, 9.19; N, 10.89; S, 8.32; HRMS for $C_{18}H_{12}ClN_3O_3S$ Calculated $[M^+]$ m/z 385.8220, Found 385.8222.

N-(benzo [*d*] thiazol-2-yl)-7-fluoro-2-hydroxy-6-methoxyquinoline-4-carboxamide (6j): Chalky white solid; Melting point: 136–138 °C: IR (KBr): 3167, 3089, 3024, 2976, 2819, 2364, 1739, 1584, 1466, 1434, 1388, 1266, 1234, 1120, 898, 764, 686, 678, 664, 646 cm^{-1}: ^1H NMR (400 MHz, $CDCl_3$) δ ppm: 12.63 (s, 1H), 11.25 (s, 1H), 8.83–8.79 (d, J = 8.0, 1H), 8.43–8.39 (t, J = 9, 1H), 8.09–8.08 (t, J = 4, 1H), 7.55–7.44 (m, 4H), 3.73 (s, 3H); ^{13}C NMR (100 MHz, $CDCl_3$) δ ppm: 175.4, 171.1, 166.4, 154.3, 145.2, 141.3, 140.1, 139.3, 138.2, 136.1, 127.0, 126.9, 126.2, 125.8, 124.7, 124.0, 123.7, 114.0, 111.0, 96.4, 57.7; Elemental Analysis, calculated: C, 58.53; H, 3.27; F, 5.14; N, 11.38; S, 8.68; Obtained: C, 58.54; H, 3.28; F, 5.14; N, 11.39; S, 8.69; HRMS for $C_{18}H_{12}FN_3O_3S$ Calculated $[M^+]$ m/z 369.3704, Found 369.3706.

N-(benzo [*d*] thiazol-2-yl)-2-hydroxy-6,7-dimethylquinoline-4-carboxamide (6k): Grey color solid; Melting point: 124–126 °C: IR (KBr): 3248, 3067, 3084, 3002, 2924, 2867, 2327, 1738, 1542, 1426, 1445, 1314, 1234, 1208, 1124, 884, 852, 796, 682, 668, 640 cm^{-1}: ^1H NMR (400 MHz, $CDCl_3$) δ ppm: 12.49 (s, 1H), 11.42 (s, 1H), 8.95 (s, 1H), 8.55–8.48 (m, 1H), 8.40–8.31 (m, 1H), 7.43–7.33 (m, 3H), 7.26 (s, 1H), 2.53 (m, 3H), 2.35 (s, 3H); ^{13}C NMR (100 MHz, $CDCl_3$) δ ppm: 178.7, 172.5, 168.5, 159.1, 156.0, 148.8, 146.5, 137.6, 132.4, 131.8, 129.1, 129.0, 128.2, 127.8, 127.0, 126.9, 118.6, 118.4, 114.7, 110.9, 110.2, 19.9, 17.9; Elemental Analysis, calculated: C, 65.31; H, 4.33; N, 12.03; S, 9.18; Obtained: C, 65.31; H, 4.33; N, 12.03; S, 9.18; HRMS for $C_{19}H_{15}N_3O_2S$ Calculated $[M^+]$ m/z 349.4080, Found 349.4082.

N-(benzo [*d*] thiazol-2-yl)-7-chloro-2-hydroxy-6-methylquinoline-4-carboxamide (6l): Brownish solid; Melting point: 128–130 °C: IR (KBr): 3298, 3112, 3016, 2984, 2892, 2346, 1764, 1538, 1424, 1408, 1342, 1234, 1206, 1122, 898, 756, 698, 676, 664, 646 cm^{-1}: ^1H NMR (400 MHz, $CDCl_3$) δ ppm: 12.66 (s, 1H), 11.11 (s, 1H), 8.99 (s, 1H), 8.13–8.04 (m, 1H), 7.93–7.74 (m, 1H), 7.43 (s, 1H), 7.41–7.36 (m, 3H), 2.26 (s, 3H); ^{13}C NMR (100 MHz, $CDCl_3$) δ ppm: 179.1, 174.5, 169.1, 157.4, 156.0, 154.0, 146.8, 138.5, 130.5, 129.5, 128.8, 128.5, 128.4, 128.2, 127.5, 125.9, 120.6, 119.6, 115.7, 112.6, 111.1, 109.8, 20.3; Elemental Analysis, calculated: C, 58.46; H, 3.27; Cl, 9.59; N,

11.36; S, 8.67; Obtained: C, 58.47; H, 3.28; Cl, 9.59; N, 11.37; S, 8.68; HRMS for $C_{18}H_{12}ClN_3O_2S$ Calculated [M^+] *m/z* 369.8230, Found 369.8233.

2.3. Cell lines preparation

The early passage of MCF-7 (Breast cancer), HCT-116 (Colon cancer), PC-3 & LNCaP (Prostate) and SK-HEP-1 (Liver cancer) cell lines used in this study were developed and cultured as previously described [17,18]. All cancer cells were cultured in DMEM (Dulbecco's Modified Eagle's Medium) supplemented with 10% Fetal Bovine Serum (FBS), (100U) 20 µg/ml penicillin, and 100 µg/ml streptomycin. They were sub-cultured by removing existing medium and adding fresh 0.25% trypsin 0.53 mM EDTA for several minutes, then trypsin was removed and the culture sit at 37 °C for 10–15 min. Incubation was carried out at 37 °C in an atmosphere of 5% CO_2. For the assay, 1 ml of homogenized cell suspension was poured in each well of a microtiter plate and kept in a desiccator. After incubated for 48 h, the cells were observed for any physiological changes in an inverted microscope. 0.05 ml of test samples was liquefied in 4.95 ml of DMSO to attain a working concentration of 1 mg/ml.

2.4. MTT assay

The anticancer activity of N-(benzo[*d*]thiazol-2-yl)-2-hydroxyquinoline-4-carboxamides (**6a-l**) on various cancer cell lines was determined by the MTT (3-(4, 5-dimethylthiazol-2yl)-2,5-diphenyl tetrazolium bromide) assay as we previously reported [17–19]. About 5000 cells were seeded in 96-well flat-bottom titer plates and then incubated for 24, 48, and 72 h in presence 5% CO_2 atmosphere and 37 °C temperature. The drug candidates **6a-l** in different concentration (10–150 µg/mL) were added into the 96-well titer plate and incubated further at different time periods. After completion of the incubation, the medium was removed from the wells. The wells were then washed with PBS; 100 µl of the working MTT dye in DMEM (Dulbecco's Modified Eagle's Medium) media was added and incubated for another 2 h. MTT lysis buffer (100 µl) was added and incubation was continued for at least 4 hrs. The absorbance was measured at 570 nm and the cell viability was calculated using the following formula

$$\text{Cell viability (\%)} = \text{Mean OD/Control OD} \times 100\%$$

2.5. hGC-ALP activity assay

The protocol for executing the hGC-ALP assay was adopted from our earlier report [20]. Generally, ALP catalyzes the hydrolysis of phosphate esters in an alkaline buffer and generating organic radical and inorganic phosphate. The changes in alkaline phosphatase quantity and activity are associated with numerous disease states (especially in the liver and bone). Thus, transphosphorylation buffers are widely used in ALP inhibition investigations. These are enabling the "double displacement" reaction mechanism of ALP [21–23]. The ALP assay kit which was used in this study uses *p*-nitrophenyl phosphate (*p*NPP*)* as a phosphatase substrate which turns yellow (λ_{max} = 405 nm) when dephosphorylated by ALP. Serum and plasma are carefully diluted up to 10 times; to measure the intracellular ALP (isozyme origin: human Germ cell ALP (hGC-ALP)), the washed cells (1 × 105) are homogenized in the assay buffer and centrifuged to remove insoluble substances at 13,000 rpm for 5 min. The range of volume of prepared candidate drug samples was loaded into the 96-well plate wells.

A centralized total volume of the reaction mixture was brought to 100 µl by adding assay buffer. To attain this, 10–50 µl (5 fold (10 mg/mL) solution) of **6a-l** in different concentrations was added to separate wells, bring volume to 80 µl. and 20 µl stop solution was added and assorted well to avoid ALP activity in the samples. Then, 75 µl of the 5 mM pNPP solution was added to each well comprising **6a-l** in different concentrations. Due to the colored samples are anticipated to obstruct with OD. 405 nm readings, distilled water was served as background control. Consequently, 75 µl distilled water was added to all wells and mixed thoroughly. This was then incubated for 75 min at 22–25 °C in dark. OD was measured at every 15 min up to eight gradual intervals. ALP activity of the test samples can then be calculated:

$$\text{ALP activity (U/ml)} = \text{Amount of pNPP generated by sample } (\mu\text{mol})/\text{Sample Volume (mL)}/\text{Reaction Time (minutes)}$$

2.6. Molecular docking studies

Docking study performed in order to get more insight into the binding mode of the PQPDs into the binding pockets of PI3 Kinase. Autodock4.2.6 and Autodock Tools (ADT)1.5.6. and the Arguslab version 4.0.1 was used for the docking studies. All strategy and measures for docking studies were followed and customized accordingly to our previous reports [24–26]. Their 3D atomic coordinates of N-(benzo[*d*]thiazol-2-yl)-2-hydroxyquinoline-4-carboxamides (**6a-l**) were created using ACD/Labs – Chemsketch 12.0 software. Compound **6a-l** geometries were cleaned and generated as the corresponding *pdb*. Ligand files. 3D crystal structure of human placental alkaline phosphatase (ALP) (they are also known as germ cell like ALP) (PDB ID: 1EW2) retrieved from the protein data bank (PDB) (Source: www.rcsb.org/pdb/). Statistical mechanical analysis for the ligands **6a-l** was analyzed and the lowest binding energy, ligand efficiency, and the inhibitory constant (*ki*) values were extracted. Molecular interactions like hydrogen bonding, π-π interaction and π-cation interaction results were analyzed and validated for structure-activity relationships.

2.7. Statistical analysis

All results were expressed as the percentage decrease with respect to control values and compared by one-way ANOVA with Dunnett's post test was performed. GraphPad Prism version 6.07 for Windows, GraphPad Software, San Diego California USA, www.graphpad.com was used for statistical analysis. A difference was considered statistically significant if $p \leq 0.05$.

3. Results and discussions

3.1. Synthesis of N-(benzo[d]thiazol-2-yl)-2-hydroxyquinoline-4-carboxamides (6a-l)

In the present study, the chemical reaction using different Lewis acids entry and bifunctional organocatalysts were used to obtain novel N-(benzo[*d*]thiazol-2-yl)-2-hydroxyquinoline-4-carboxamides (**6a-l**) in higher yield using substituted acetoacetanilides (Scheme 1). Among the range of solvents used, the use of *p*-TSA·H_2O enhanced the reactivity, a lesser amount of reaction time and higher amount of yield deprived of purification over tiresome column chromatography technique. The maximum quantity of treatment of *p*-TSA·H_2O essential for this reaction was adjusted (15 mol %) in order to reduce excess catalyst usage. However, inappropriately, diminishing the catalyst amount reduced the yield of compounds **6j**, **6 k**, and **6 l**. Later, the use of 15 mol percentage of *p*-TSA·H_2O in water was able to provide satisfaction with a high reaction yield of **6f** (98%). Furthermore, the influence of different solvent usage was also examined in order to optimize the product yield in lesser reaction time. Quite a few numbers of organic solvents such as methanol (MeOH), CH_3CN and showed no significant to ethanol (EtOH) that in turn has also no imperative to *P*-TSA·H_2O, has given high reaction yield of **6 l** (95%).

Initially, the reaction of 2-hydroxyquinoline-4-carbonyl chloride (**4**) was started with substituted acetoacetanilides having electron donating

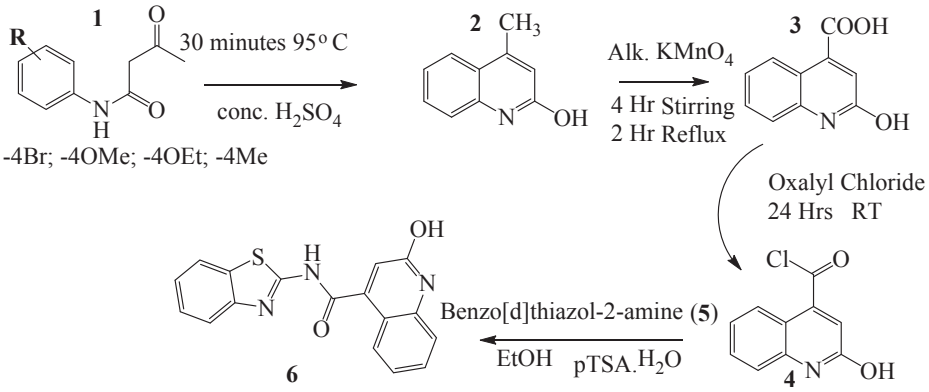

Scheme 1. Route of synthesis of N-(benzo[*d*]thiazol-2-yl)-2-hydroxyquinoline-4-carboxamides (**6a-l**).

entities like −4Br; −4OMe; −4OEt; −4Me groups that are having solid electron-withdrawing potency were reacted in quicker rates of chemical association and dissociation processes after the addition of different catalysts compared with that substituted acetoacetanilide reaction in the usual solvent conditions. In general, all compounds were able to synthesize in presence different catalyst using eco-friendly ethanol (EtOH) as a solvent. While loading 10% catalyst ($SnCl_2{\cdot}H_2O$, *p*-TSA·H_2O) to **6b** and **6i** were not able to synthesize in higher yields. Thus, we increased the catalyst addition up to 15–20% produced a significant yield of the compounds **6b**, 84% and **6i**, 98% in the presence of *p*-TSA·H_2O.

Compounds **6c**, **6j** was synthesized with a catalyst percentage range of 5–20 % mol $AlCl_3$ (20%), *p*-TSA·H_2O (15%) given a moderate to good yield of compounds **6c** (76%) and **6j** (96%) and **6d**, **6k** $FeCl_3$ (20%) *p*-TSA·H_2O (15%) produced a remarkable yield of 92% and 96% correspondingly. Meanwhile, compounds **6e** and **6l** were synthesized using the L-proline, $SnCl_2{\cdot}H_2O$ (25% mol) as catalyst was also produced a moderate to the respectable yield of 70 and 98% respectively. In the end, compounds **6j**, **6g**, **6l,** and **6n** were synthesized using *p*-TSA·H_2O (catalyst range of 5–20 mol %) produced a maximum yield of 96% (**6j**). In the investigation of reaction, properties/effect of different organic solvents like MeOH and CH_3CN showed no dominance to EtOH. In the meantime, the same reactions accomplished in the presence of water produced tremendous yield within 2–6 h.

3.2. Evaluation of alkaline phosphatase (ALP) inhibitory potentials

Initially, through a competitive ELISA colorimetric assay, the essential diagnostic screen of N-(benzo[*d*]thiazol-2-yl)-2-hydroxyquinoline-4-carboxamides (**6a-l**) against hGC-ALP assessed. Not only to unveil the hGC-ALP inhibition prospective of **6a-l**, but the main purpose of hGC-ALP inhibition assay is to segregate the most effective compounds among hydroxyquinoline-carboxamides (**6a-l**) in order to develop them as anti-prostate cancer drugs. Because of the straight association between hGC-ALP and prostate cancer already revealed. Therefore, screening the utmost and appropriate candidate drugs was deliberated here, not only for limiting the essential research interlude but also to keep an economical way of drug development processes. Fig. 3A–C illustrates the results of hGC-ALP inhibition assay.

Based on the results the best compounds were screened for further anticancer studies by comparing with standard (Estradurin). Obviously, the results were found in a dose-dependent manner. For authorizing or screening the most effective hGC-ALP inhibitors among **6a-l**, a relative % activity along with the IC_{50} values was considered and according to the values the compounds were ranked from best to worst. In the assessments, **6d, 6i, 6k,** and **6l** were found with the smallest amount of IC_{50} values < 0.075 μM (Fig. 3A) with a highest relative activity of 92%, 90%, and 96% respectively (Fig. 3B). The IC_{50} of compounds **6h, 6i,** and **6k** found between 0.05 and 0.15 μM ranges. **6d** and **6g-l** were showed excellent inhibition potential than the standard, Estradurin (82% of the relative activity with an IC_{50} 1.5 μM).

Fig. 3C illustrates the dose–response inhibition activity of for the most potent compounds **6l** and the standard Estradurin. As **6l** started to show maximum inhibition from 10^{-4} and lasted up to 10^{-7} (μg/mL), its stability was recognized while Estradurin showed maximum activity only at the concentrations 10^{-5} and 10^{-6} (μg/mL). Among all, **6a-c** and **6f** found with lesser or no hGC-ALP inhibition activity. Simultaneously, we have screened compounds **6d** and **6g-l** for further anti-prostate cancer evaluations as they exhibited excellent hGC-ALP inhibition as well as firm interaction to the human Placental ALP (hP-ALP) binding pocket (Fig. 3D). Both ALP are highly resemble structurally and functionally.

3.3. Molecular docking studies – assessment of receptor-ligand interaction

To get more insight into the molecular level interaction of present study N-(benzo[*d*]thiazol-2-yl)-2-hydroxyquinoline-4-carboxamides (**6a-l**), these compounds were docked into the active sites of human placental ALP (PDB ID: 1EW2) which is highly relevant to Human Germ Cell ALP. Molecular mechanistic values were retrieved from best-docked poses such as lowest binding affinity, least binding energy, and ligand efficiency. Molecular interactions by means of non-covalent bonding such as π-π interaction and π-cation interaction along with hydrogen bonding interactions were verified. In the results, expected binding free energy values of ALP was established in −6.28 to −10.79 kcal/mol and inhibitory constant (*ki*) were found in the range of 0.005–5 μM (Fig. 4A–D).

As emphasized in yellow (Fig. 4A), compounds **6d,** and **6g-l** were showed the most prominent results. There were a correlation between the molecular docking (*in silico*) values to ALP inhibition (*in vitro*), thus the progress of the present research was evenly poised and given away for screening pre-eminent compounds for evaluating anti-prostate cancer studies were screened. Furthermore, for the comparison purpose, molecular docking was conducted for also to Estradurin, the standard drug used for the ALP assay. Among **6a-l**, except **6e**, remaining compounds showed dominated molecular mechanistic values as displayed in Fig. 4A.

3.3.1. Receptor-Ligand interface assessments by molecular docking simulations

Docking simulation is the process of assessment of interactions between Ligand & Receptor. As displayed in Fig. 4B–C, these two compounds found to have all expected interactions such as non-covalent bonding (π-π interaction) and hydrogen bonding. All hydrogen bonding were established within 1.5 Å to the 2.1 Å range. Estradurin, the standard ALP inhibitor established hydrogen bonds with Arg166 (1.587 Å), Asp42 (2.063 Å), His153, 432 (2.188 Å), Ser92 (1.693 Å) (Fig. 4D). As displayed in Fig. 4B, compound **6k** found to have both hydrogen bond

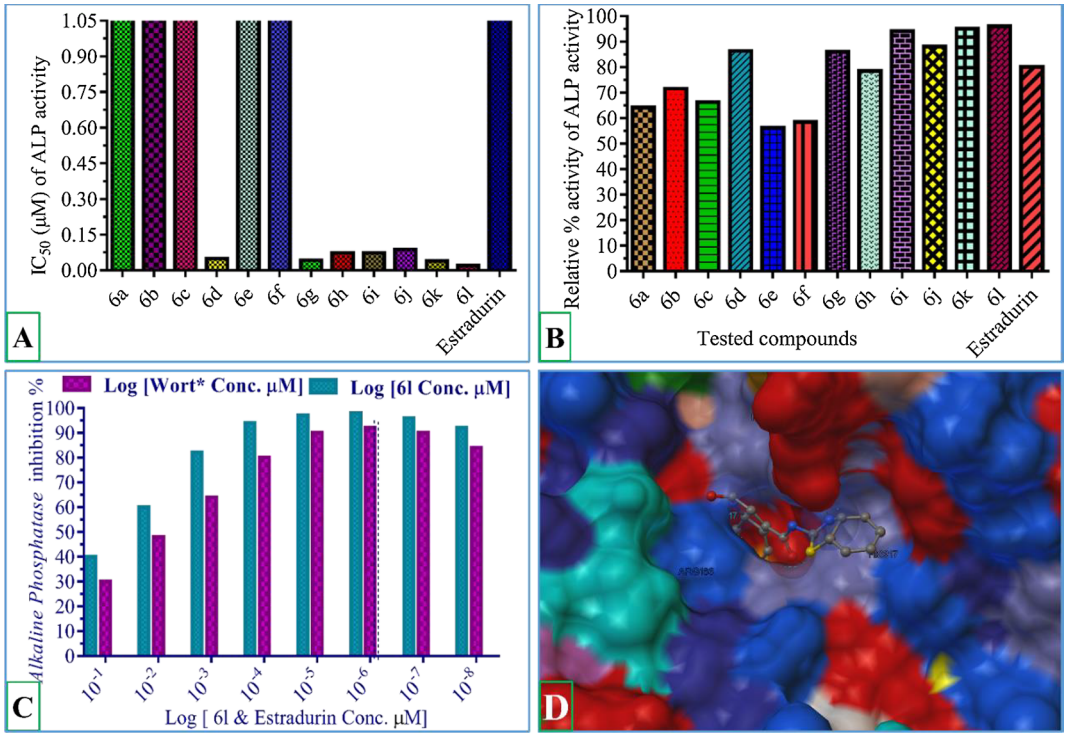

Fig. 3. Results of hGC-ALP inhibition by **6a-l**. Results are the average of duplicate or triplicate values. Fig. 3C. Dose-response curve of **6l,** and Estradurin. Results are the average of duplicate or triplicate values.

with key amino acid residues (Arg166 (2.145 Å); His432 (1.923 Å) and Glu428) and non-covalent bond (π-π interaction between quinoline aryl ring to His153). Compound **6 l** also established with as many hydrogen bonds along with the anticipated key amino acid residues (Arg166 (2.017 Å); His153 (2.058 Å) and His432 (1.887 Å)) as well as with few others (His317 (2.083 Å) and His320 (1.761 Å)). In the plausible mechanism, His432 probably donates an electron to the quinoline carboxylic oxygen end, where the $-O^-$ is present in compound **6k** and **6l**. Hence, a conceivable $-NH_2-O^-$ complex could be recognized which enables the ALP inhibition promising.

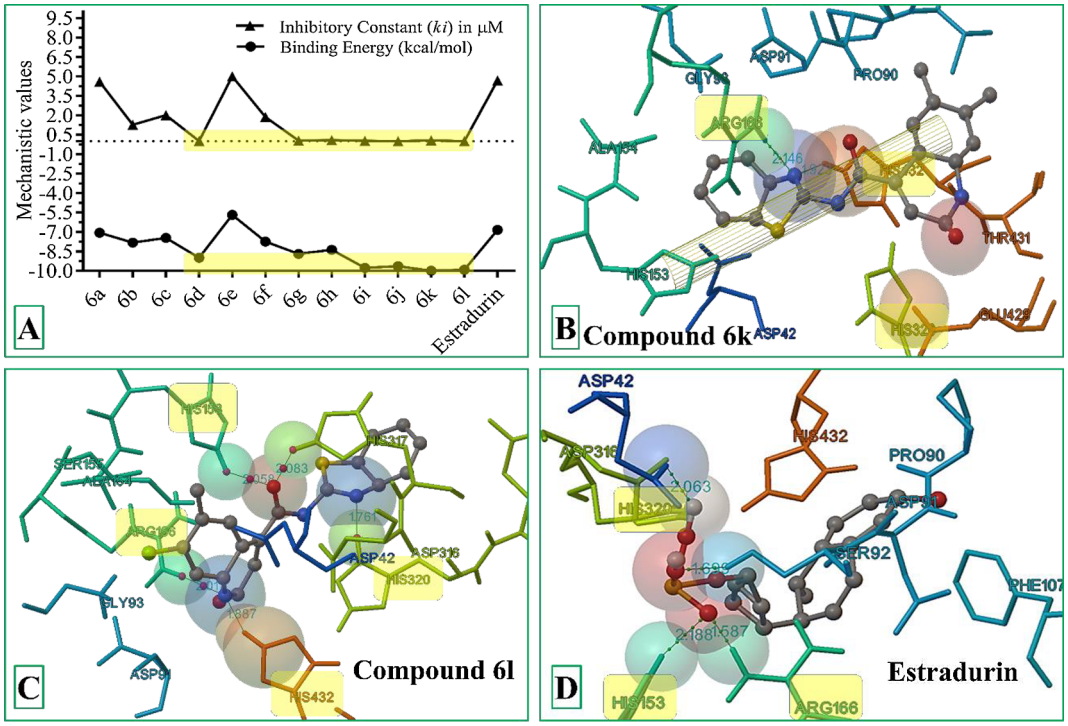

Fig. 4. Molecular mechanistic values of **6a-l** to Human Placental ALP (PDB ID: 1EW2) (values are the average of three repeated docking processes). Yellow highlight in (A) indicates the most desirable docking values. Yellow rectangle highlighted indicates the key amino acid comparison with compound **6k** (B), **6l** C) and Estradurin (D).

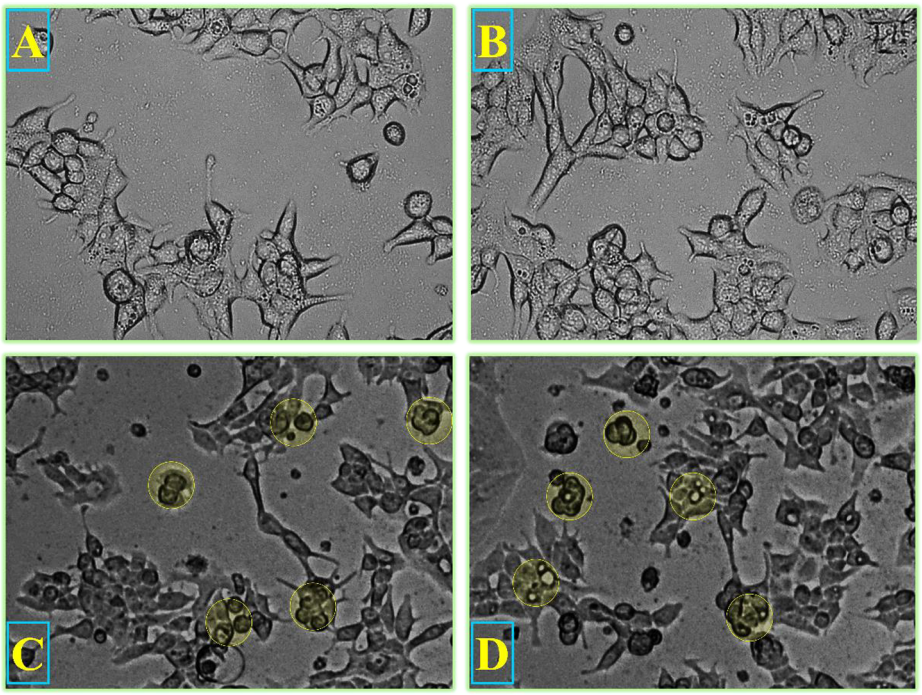

Fig. 5. Anticancer effect of **6i** and **6l** against PC-3 cell lines. PC-3-a control treated (Distilled water); PC-3-b standard (Estradurin) treated; PC-3-c compound **6i** treated and PC-3-d compound **6l** treated. Yellow circle mark indicates the necrosis generated due to the drug/compound action.

3.4. Anticancer activity evaluations

The anti-prostate cancer drug efficacy of **6k** and **6l** through ALP inhibition mechanism was recognized through in silico and *in vitro* studies. In the activity, among all the cell lines used, compounds **6k** and **6l** were found with the selective anti-proliferative activity mostly on both the cancer cells (PC-3 and LNCaP). In the meantime, there was no activity was found (up to 150 μg/ml) against normal epithelial (MCF-10) cell lines. The IC_{50} values found for compounds **6k** (0.048 ± 0.002 μM) and **6l** (0.018 ± 0.002 μM) designate them as more active than the standard Bicalutamide (CDX) (1.3 ± 0.08 μM). The relative % activity was 92.26 ± 1.12%, 94.45 ± 1.08%, and 88.24 ± 2.04% respectively for **6k**, **6l** and Bicalutamide (CDX). Fig. 5A–D shows the anticancer effects before (Fig. 5A&B) and after (Fig. 5C&D) treating the compounds **6k** and **6l** on PC-3 cell lines. There was significant necrosis found on PC-3 cell lines after treating (2 h) **6k** (Fig. 5C) and **6 l** (Fig. 5D).

3.5. Results of HRBC membrane stabilization potential of 6a-l

Compounds **6k** and **6l** were taken to measure the inflammation preventing capacities through the inhibition of HRBC membrane lysis on Hypotonicity induced red blood cells. In the results, both compounds were showed no toxic effect even after the maximum concentration (150 μg/mL) used in this study. compound **6k** showed a maximum protective effect up to 96.12 ± 0.80% with an IC_{50} 0.022 ± 0.002 μM, and **6l** showed 98.34 ± 0.92%) while the standard Diclofenac showed up to 90.22 ± 1.02% (IC_{50} 1.0 ± 0.02 μM).

3.6. Druggability assessments of hydroxyquinoline-4-carboxamides (6a-l)

Table 1 depicts the centralized three repeated predicted values of ADMET properties of **6a-l**. There were no compounds found violating the druggability properties as they showed affordable values. Especially the potentially identified ALP inhibitors **6k** and **6l** had affordable MlogP values (2.5 and 2.8 respectively) which ensure less lipophilicity.

3.7. Structure-Activity relationships

In order to recognize the Structure-Activity Relationship (SAR) primarily, effectively synthesized novel N-(benzo[*d*]thiazol-2-yl)-2-hydroxyquinoline-4-carboxamides (**6a-l**) with a wide range of electron withdrawing and electron discharging groups R_1 position of quinoline ring were synthesized and established as active drug candidates against prostate cancer tested on PC-3 and LNCaP prostate cancer cell lines. Effective molecular interaction (verified through molecular docking studies) ALP inhibition (validated through *in vitro* Human Germ Cell ALP assay), potential compounds **6k** (substituted with −S, −Cl, $-CH_3$, −OH along with carbonyl and amides), and **6l** (substituted with −S, $-CH_3$, $-CH_3$, −OH along with carbonyl and amides) in the inhibition of alkaline phosphatase were recognized. Fig. 6 exemplifies the plausible mechanism of action of ALP inhibition by the compound **6 l**.

4. Conclusions

In the present study, novel N-(benzo[*d*]thiazol-2-yl)-2-hydroxyquinoline-4-carboxamides (**6a-l**) were synthesized and their anti-prostate cancer efficacy was recognized through ALP inhibition potentials. The synthetic reaction carried out in ethanol in the presence of a different bio-friendly catalyst. In the product development, we used only simple filtration and extraction and remarkably not the tedious chromatographic techniques. In conclusion, novel N-(benzo[*d*]thiazol-2-yl)-2-hydroxyquinoline-4-carboxamides (**6a-l**) were efficaciously synthesized as ALP inhibitors so as the anti-prostate cancer agents by means of ecologically friendly catalytic systems in very good yields. The therapeutic solicitations of the compounds were examined and attained the following verdicts

- As the interrelation between Human Germ Cell ALP and prostate cancer was systematically assessed and related.
- Compounds **6k** and **6l** were showed potent Human Germ Cell ALP enzyme inhibition activity and anti-prostate cancer effects.

With these positive results, currently taking forward the *in vivo*

Table 1
ADMET assessments data of hydroxyquinoline-4-carboxamides (**6a-l**).

Name	DiffCoef	MlogP	RO5	RO5_Code	MWt	M_NO	T_PSA	HBDH
6a	0.755	2.587	0	< None >	355.804	5	75.11	2
6b	0.746	2.704	0	< None >	400.26	5	75.11	2
6c	0.776	2.469	0	< None >	339.35	5	75.11	2
6d	0.771	1.578	0	< None >	337.359	6	95.34	3
6e	0.741	1.815	0	< None >	351.386	6	84.34	2
6f	0.714	2.048	0	< None >	365.413	6	84.34	2
6g	0.633	−0.113	0	< None >	459.502	9	138.71	3
6h	0.722	1.567	0	< None >	366.4	7	110.36	4
6i	0.718	2.048	0	< None >	385.831	6	84.34	2
6j	0.736	1.932	0	< None >	369.376	6	84.34	2
6k	0.722	2.552	0	< None >	349.413	5	75.11	2
6l	0.727	2.82	0	< None >	369.831	5	75.11	2

Notes: MlogP. Moriguchi estimation of logP. HBDH. A number of Hydrogen bond donor protons. M_NO. A total number of Nitrogen and Oxygen atoms. T_PSA. The topological polar surface area in square angstroms. Ro5 - Rule Of Five. Rule Of Five_Code. Hb = number of Hydrogen bond donor protons; Mw = molecular weight; NO = number of Nitrogen- and Oxygen-based Hydrogen bond acceptors.

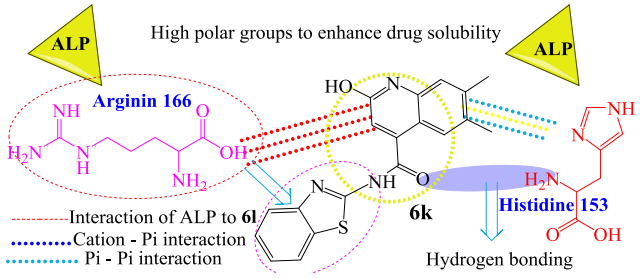

Fig. 6. The plausible mechanism proposed for compound **6k** – Human Germ Cell ALP interaction.

studies in animal models only for the potentially identified and most efficacious compounds **6k,** and **6l**.

Appendix A. Supplementary material

Supplementary data to this article can be found online at https://doi.org/10.1016/j.bioorg.2019.103171.

References

[1] B. Soni, M.S. Ranawat, R. Sharma, A. Bhandari, S. Sharma, Synthesis and evaluation of some new benzothiazole derivatives as potential antimicrobial agents, Eur. J. Med. Chem. 45 (2010) 2938–2942.

[2] S. Bondock, W. Fadaly, M.A. Metwally, Synthesis and antimicrobial activity of some new thiazole, thiophene and pyrazole derivatives containing benzothiazole moiety, Eur. J. Med. Chem. 45 (9) (2010) 3692–3701.

[3] P.C. Sharma, A. Sinhmar, A. Sharma, H. Rajak, D.P. Pathak, Medicinal significance of benzothiazole scaffold: an insight view, J. Enzyme Inhib. Med. Chem. 28 (2013) 240–266.

[4] M. Robert, An overview of quinoline as a privileged scaffold in cancer drug discovery, Expert Opin. Drug Discov. 12 (2017) 583–597.

[5] B.M. Sheetal, R.K. Ravindra, H. Joy, D. Jagadish Prasad, Y.M. Gangadhar, Med. Chem. Res. 23 (2014) 2727.

[6] F.K. Abdel-Wadood, M.I. Abdel-Monem, A.M. Fahmy, A.A. Geies, Synthesis, reactions, and biological activities of some new thieno[3,2-c]quinoline and pyrrolo[3,2-c]quinoline derivatives, Arch Pharm. (Weinheim). 347 (2014) 142–152.

[7] M. Vikramdeep, N. Amit, V. Balasubramanian, P.B. Prakash, J. Sarbjit Singh, K. Sukhraj, P.S. Prati, R. Jain, Synthesis and antimycobacterial activities of ring-substituted quinolinecarbohydrazide and ring-substituted quinolinecarboxamide analogs, Biorg. Med. Chem. 12 (2004) 6465–6472.

[8] C.H. Tseng, Y.L. Chen, P.J. Lu, C.N. Yang, C.C. Tzeng, Synthesis and antiproliferative evaluation of certain indeno[1,2-c]quinoline derivatives, Bioorg. Med. Chem. 16 (2008) 3153–3162.

[9] Y.L. Zhao, Y.L. Chen, F.S. Chang, C.C. Tzeng, Synthesis and cytotoxic evaluation of certain 4-anilino-2-phenylquinoline derivatives, Eur. J. Med. Chem. 40 (2005) 792–797.

[10] S.C. Kuo, H.Z. Lee, J.P. Juang, Y.T. Lin, T.S. Wu, J.J. Chang, D. Lednicer, K.D. Paull, C.M. Lin, E. Hamel, K.H. Lee, Synthesis and cytotoxicity of 1,6,7,8-substituted 2-(4'-substituted phenyl)-4-quinolones and related compounds: identification as antimitotic agents interacting with tubulin, J. Med. Chem. 36 (1993) 1146–1156.

[11] Y. Xia, Z.Y. Yang, P. Xia, K.F. Bastow, Y. Tachibana, S.C. Kuo, E. Hamel, T. Hackl, K.H. Lee, Synthesis and biological evaluation of 6,7,2',3',4'-substituted-1,2,3,4-tetrahydro-2-phenyl-4-quinolones as a new class of antimitotic antitumor agents, J. Med. Chem. 41 (1998) 1155–1162.

[12] G.L. Firestone, S.N. Sundar, Anticancer activities of artemisinin and its bioactive derivatives, Expert Rev. Mol. Med. 11 (2009) e32.

[13] J.J. Lu, L.H. Meng, Y.J. Cai, Q. Chen, L.J. Tong, L.P. Lin, Dihydroartemisinin induces apoptosis in HL-60 leukemia cells dependent on iron and p38 mitogen-activated protein kinase activation but independent of reactive oxygen species, Cancer Biol. Ther. 7 (2008) 1017–1023.

[14] V.V. Kouznetsov, F.A. Rojas Ruíza, L.Y. Vargas Méndeza, M.P. Gupta, Simple C-2-Substituted Quinolines and their Anticancer Activity, Lett. Drug Des. Discovery 9 (2012) 680–686.

[15] T. Yadagiri, A. Mahesh, T. Prakruti, G. Balaram, J. Mukund, B. Anupam, Synthesis and anti-cancer activity of 1,4-disubstituted imidazo[4,5-c]quinolines, Org. Biomol. Chem. 14 (2016) 876–883.

[16] Y. Mikata, Y. Mika, O. Shun-Ichiro, O. Ichiro, M. Kawasaki, M. Maeda, Y. Shigenobu, Effect of side chain location in (2-aminoethyl)aminomethyl-2-phenylquinolines as antitumor agents, Bioorg. Med. Chem. Lett. 8 (1998) 1243–1248.

[17] A. Manikandan, A. Sivakumar, Molecular explorations of substituted 2-(4-phenylquinolin-2-yl) phenols as phosphoinositide 3-kinase inhibitors and anticancer agents, Cancer Chemother. Pharmacol. 79 (2017) 389–397.

[18] P. Thangarasu, S. Thamaraiselvi, A. Manikandan, Unveiling novel 2-cyclopropyl-3-ethynyl-4-(4-fluorophenyl)quinolines as GPCR ligands via PI3-kinase/PAR-1 antagonism and platelet aggregation valuations; Development of a new class of anticancer drugs with thrombolytic effects, Bioorgan. Chem. 81 (2018) 468–480.

[19] O. Tacar, P. Sriamornsak, C.R. Dass, Doxorubicin: an update on anticancer molecular action, toxicity, and novel drug delivery systems, J. Pharm. Pharmacol. 65 (2) (2013) 157–170.

[20] M. Rajesh Kumar, A. Manikandan, A. Sivakumar, D. Violet, An eco-friendly catalytic system for multicomponent, one-pot synthesis of novel spiro-chromeno indolinetriones and their anti-prostate cancer potentials evaluated via alkaline phosphatase inhibition mechanism, Bioorg. Chem. 81 (2018) 44–54.

[21] R.M. Bell, D.E. Koshland Jr., Covalent Enzyme-Substrate Intermediates, Science 172 (1971) 1253–1256.

[22] G.N. Bowers Jr., R.B. McComb, Measurement of total alkaline phosphatase activity in human serum, Clin. Chem. 21 (1975) 1988–1995.

[23] J.L. Millán, Alkaline Phosphatases; Structure, substrate specificity and functional relatedness to other members of a large superfamily of enzymes, Purinergic Signal. 2 (2006) 335.

[24] A. Manikandan, V.P. Muralidharan, M. Andrew, M.H. Ahmed, S.K. Iyer, A. Sivakumar, Computational Approaches to Develop Isoquinoline Based Antibiotics through DNA Gyrase Inhibition Mechanisms Unveiled through Antibacterial Evaluation and Molecular Docking, Mol. Inf. 37 (2018) 1800048, https://doi.org/10.1002/minf.201800048.

[25] A. Manikandan, A. Sivakumar, Molecular docking, discovery, synthesis, and pharmacological properties of new 6-substituted-2-(3-phenoxyphenyl)-4-phenyl quinoline derivatives; an approach to developing potent DNA gyrase inhibitors/antibacterial agents, Bioorg. Med. Chem. 25 (2017) 1448–1455.

[26] M. Arif, F. Ozlem, D. Ahmet, D. Neslihan, A. Manikandan, A. Sivakumar, Piperazine-azole-fluoroquinolone hybrids: conventional and microwave irradiated synthesis, biological activity screening and molecular docking studies, Bioorgan. Chem. 85 (2019) 308–318.